Supplementary Information

Reactivity of Pt- and Pd-bound nitriles towards nitrile oxides and nitrones: substitution versus cycloaddition

Maxim L. Kuznetsov,[*a,b] **Vadim Yu. Kukushkin,**[c] **and Armando J. L. Pombeiro**[*a]

[a] *Centro de Química Estrutural, Complexo I, Instituto Superior Técnico, TU Lisbon, Av. Rovisco Pais, 1049-001 Lisbon, Portugal. E-mail: pombeiro@ist.utl.pt*

[b] *Department of Chemistry, Moscow Pedagogical State University, 3, Nesvigskiy per., 119021 Moscow, Russian Federation. E-mail: max@mail.ist.utl.pt*

[c] *Department of Chemistry, St. Petersburg State University, 198504 Stary Petergof, Russina Federation*

NBO and AIM analyses

Additional information about the nature of the coordination bonds may be obtained by the NBO and AIM analyses (Tables 3S and 4S). For the nitrile complexes **1** and **2**, the natural orbital for the M–N bond was detected. This bond is strongly polarized towards the nitrogen atom (ca. 82–85% at N), which is sp-hybridized, whereas the d and s orbitals of the metal are equally involved in the bond formation. All the σ- and π-natural orbitals of the CN multiple bonds of nitrile and 1,3-dipoles are clearly polarized towards the nitrogen end. On the contrary, for the substitution products, no M–O bond orbitals were found indicating a conceivable predominant Coulomb-type metal-ligand interaction. This interpretation is supported by the topological analysis of the electron density distribution (Table 4S). The energy density (H_b) at the critical point of the M–N bond has a small negative magnitude for **1** and **2** (–0.235 and –0.130 Hartree A^{-3}, respectively), what reveals some, although minor, covalent contribution to the M–N bonds.[1S] In the case of the reaction products, the H_b values of the M–O bonds are significantly closer to zero (virtually zero for **$P_{SUB-NO-2}$**) demonstrating negligible covalent contributions, and this situation is typical for the closed-shell interactions. The NBO analysis of TSs does not indicate any natural bond orbitals for the M···N and M···O contacts but the AIM calculations were able to locate the bond critical points for both these contacts (Figure 1S). Thus, the M···N and M···O contacts may be considered as greatly weakened chemical bonds, and the coordination number of the metal in TSs is five.

Reference for the Supplementary Information

1S D. Cremer, E. Kraka, *Angew. Chem., Int. Ed. Engl.*, 1984, **23**, 62.

Table 1S **Most important characteristics of the transition states**[a]

	NPA	vi	$\delta B(MO)$	$\delta B(MN)$	δB_{av}	A_s	ρ_1	ρ_2	H_{b1}	H_{b2}	μ
TS$_{CA-NO-1}$	0.19	406i				0.22	0.585	0.267	–0.123	+0.002	3.26
TS$_{CA-NO-2}$	0.18	399i				0.21	0.553	0.274	–0.105	0.000	3.38
TS$_{CA-N-1}$	0.31	263i				0.33	0.994	0.235	–0.507	+0.002	2.80
TS$_{CA-N-2}$	0.31	288i				0.31	0.965	0.249	–0.465	–0.001	2.63
TS$_{SUB-NO-1}$	0.10	166i	0.4338	0.7052	0.5695	0.24	0.272	0.287	–0.008	–0.010	2.33
TS$_{SUB-NO-2}$	0.09	133i	0.4407	0.6692	0.5550	0.21	0.250	0.266	–0.001	0.000	1.76
TS$_{SUB-N-1}$	0.11	153i	0.4536	0.6639	0.5588	0.19	0.318	0.342	–0.018	–0.017	1.02
TS$_{SUB-N-2}$	0.10	132i	0.4380	0.5940	0.5160	0.15	0.277	0.332	–0.004	0.000	1.13

[a] NPA charge transfer from the dipole to the rest part of the complex moiety (NPA, au), "imaginary" frequencies (vi), relative variations of the Wiberg bond indices for the MO(4) and MN(1) contacts ($\delta B(MO)$ and $\delta B(MN)$), average value of the relative variations of B_i (δB_{av}), asynchronicity (A_s), electron densities, in e $\mathring{A}^{-3}$, for the C(2)O(4) (CAs) or MO(4) (SUBs) (ρ_1) and N(1)C(6) (CAs) or MN(1) (SUBs) (ρ_2) contacts, energy densities (H_{b1} and H_{b2}, Hartree $\mathring{A}^{-3}$) for the corresponding contacts, and dipole moment (μ, Debye).

Table 2S NBO atomic charges on reacting atoms (eu) and the energy of the interacting LUMO and HOMO (eV) of the dipoles and complexes 1 and 2

	N(1)	C(2)	M	ε(2-LUMO)
1	–0.35	+0.47	+0.62	–0.95
2	–0.35	+0.47	+0.67	–0.75
	O(4)		C(6)	ε(HOMO)
CH$_3$C≡NO	–0.41		+0.22	–6.73
CH$_3$CH=N(CH$_3$)O	–0.53		–0.01	–5.66

Table 3S Result of NBO analysis of the starting complexes 1 and 2 and the substitution products[a]

Bond orbital		1	2	$P_{SUB-NO-1}$	$P_{SUB-N-1}$	$P_{SUB-NO-2}$	$P_{SUB-N-2}$
M–N/O	%M	18.42; sd$^{54.60}$	14.98; sd$^{50.40}$				
	%N/O	81.58; sp$^{53.38}$	85.02; sp$^{53.70}$				
NC (σ)	%N	60.40; sp$^{46.41}$	59.92; sp$^{46.02}$	62.53; sp$^{41.54}$	63.40; sp$^{58.91}$	62.54; sp$^{41.48}$	63.36; sp$^{58.76}$
	%C	39.60; sp$^{54.82}$	40.08; sp$^{54.72}$	37.47; sp$^{57.67}$	36.60; sp$^{69.22}$	37.46; sp$^{57.56}$	36.64; sp$^{69.07}$
NC (π)	%N	59.79; p$^{99.81}$	59.08; p$^{99.78}$	59.90; p$^{99.87}$	64.99; p$^{99.45}$	59.79; p$^{99.87}$	65.13; p$^{99.63}$
	%C	40.21; p$^{99.84}$	40.92; p$^{99.85}$	40.10; p$^{99.81}$	35.01; p$^{99.58}$	40.21; p$^{99.82}$	34.87; p$^{99.70}$
NC (π)	%N	60.00; p$^{99.81}$	59.53; p$^{99.79}$	62.21; p$^{99.06}$		61.86; p$^{99.21}$	
	%C	40.00; p$^{99.84}$	40.47; p$^{99.85}$	37.79; p$^{99.15}$		38.14; p$^{99.25}$	
N–O	%N			49.08; sp$^{59.37}$	48.66; sp$^{74.81}$	49.19; sp$^{59.28}$	48.92; sp$^{74.59}$
	%O			50.92; sp$^{75.31}$	51.34; sp$^{76.99}$	50.81; sp$^{75.45}$	51.08; sp$^{77.45}$

[a] Occupation of all NBO orbitals is 1.96–2.00. The hybridization is indicated with the percent contribution of d or p orbitals.

Table 4S Results of the topological analysis of the electron density distribution for the starting complexes and substitution products[a]

|	$\rho(\mathbf{r})$	$\nabla^2\rho(\mathbf{r})$	H_b
1	0.844	15.256	–0.235
2	0.714	13.856	–0.130
$\mathbf{P_{SUB-NO-1}}$	0.533	10.727	–0.032
$\mathbf{P_{SUB-N-1}}$	0.628	11.715	–0.073
$\mathbf{P_{SUB-NO-2}}$	0.480	10.141	0.003
$\mathbf{P_{SUB-N-2}}$	0.561	10.969	–0.025

[a] Electron densities ($\rho(\mathbf{r})$, e Å^{-3}), Laplacian ($\nabla^2\rho(\mathbf{r})$, e Å^{-5}), energy densities (H_b, Hartree Å^{-3}).

**Table 5S Total energies (E), enthalpies (H) and Gibbs free energies (G) (Hartree) of the calculated structures**

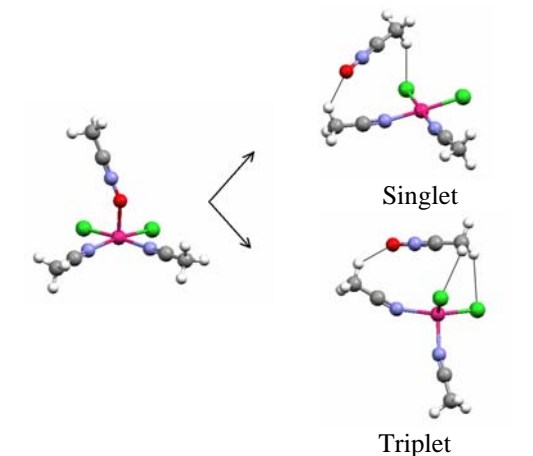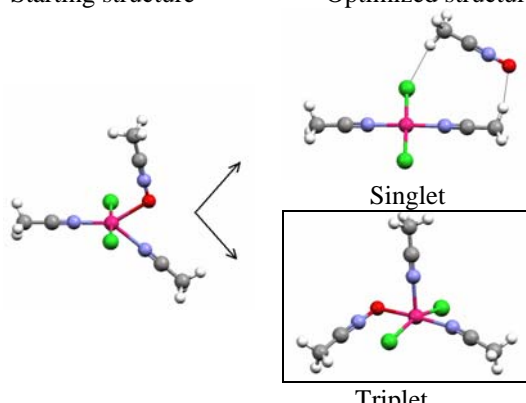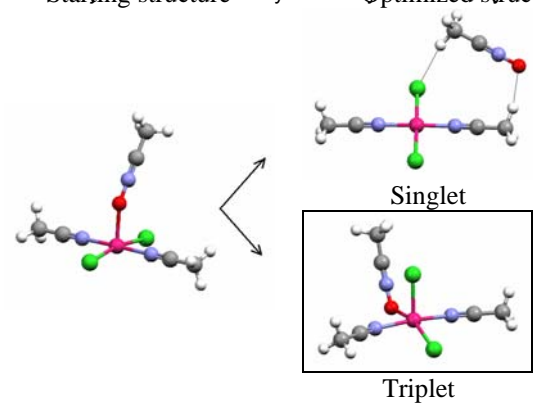|	CH$_3$C≡NO	CH$_3$CH=N(CH$_3$)O	CH$_3$C≡N	**1**	**2**
E	–207.899237	–248.435874	–132.754929	–1305.410811	–1313.941246
H	–207.843746	–248.326800	–132.704747	–1305.298316	–1313.828872
G	–207.875935	–248.362894	–132.733302	–1305.358649	–1313.889337
	P$_{CA-NO-1}$	**P$_{CA-NO-2}$**	**P$_{CA-N-1}$**	**P$_{CA-N-2}$**	**P$_{SUB-NO-1}$**
E	–1513.407051	–1521.937421	–1553.899355	–1562.429662	–1380.537777
H	–1513.235495	–1521.765048	–1553.674457	–1562.203936	–1380.420475
G	–1513.298806	–1521.832217	–1553.741684	–1562.274448	–1380.483638
	P$_{SUB-NO-2}$	**P$_{SUB-N-1}$**	**P$_{SUB-N-2}$**	**TS$_{CA-NO-1}$**	**TS$_{CA-NO-2}$**
E	–1389.074703	–1421.096606	–1429.631080	–1513.290813	–1521.822016
H	–1388.957488	–1420.925214	–1429.460746	–1513.122588	–1521.653950
G	–1389.020404	–1420.992059	–1429.524042	–1513.193342	–1521.724847
	TS$_{CA-N-1}$	**TS$_{CA-N-2}$**	**TS$_{SUB-NO-1}$**	**TS$_{SUB-NO-2}$**	**TS$_{SUB-N-1}$**
E	–1553.841672	–1562.371768	–1513.277770	–1521.821588	–1553.824998
H	–1553.618787	–1562.149958	–1513.109687	–1521.653581	–1553.602936
G	–1553.691198	–1562.219256	–1513.186864	–1521.730570	–1553.684722
	TS$_{SUB-N-2}$	**OC1$_{NO-1}$**	**OC2$_{NO-1}$**	**OC1$_{NO-2}$**	**OC2$_{NO-2}$**
E	–1562.367532	–1513.323546	–1513.305950	–1521.854014	–1521.842255
H	–1562.145643	–1513.153665	–1513.137452	–1521.685207	–1521.672895
G	–1562.225728	–1513.232856	–1513.211434	–1521.758905	–1521.751310
	OC1$_{N-1}$	**OC2$_{N-1}$**	**OC1$_{N-2}$**	**OC2$_{N-2}$**	
E	–1553.862520	–1553.864318	–1562.392783	–1562.399838	
H	–1553.639653	–1553.641648	–1562.169105	–1562.176354	
G	–1553.715509	–1553.719952	–1562.248111	–1562.254886	
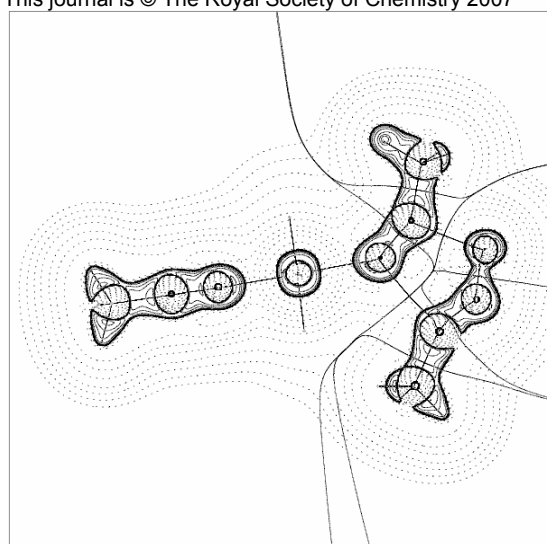
$$TS_{CA-NO-2}$$
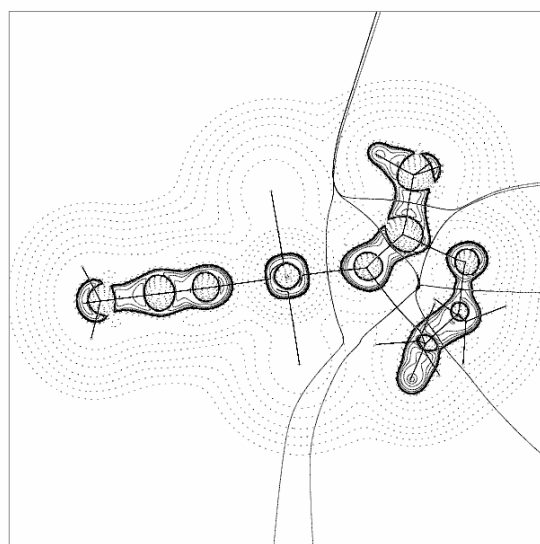
$$TS_{CA-N-2}$$
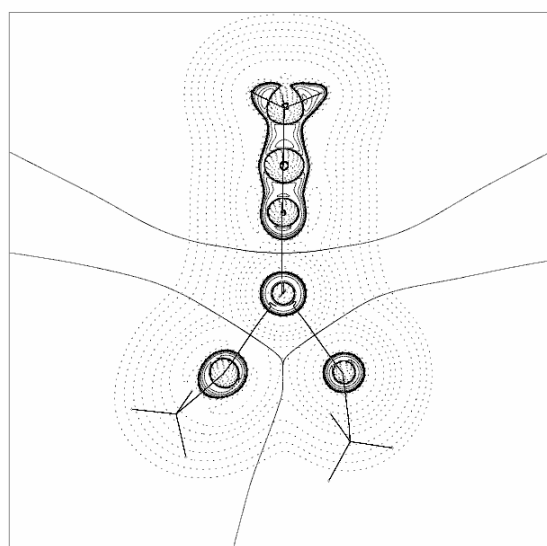
$$TS_{SUB-NO-2}$$
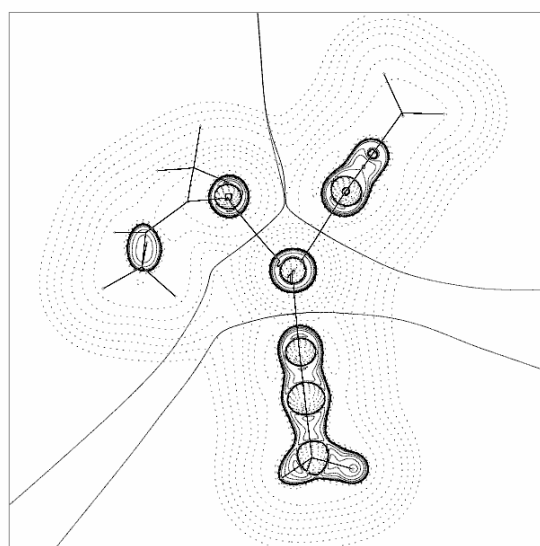
$$TS_{SUB-N-2}$$

Figure 1S Contour line diagrams of the Laplacian distribution $\nabla^2\rho(\mathbf{r})$, bond paths and selected zero-flux surfaces for $TS_{CA-NO-2}$, TS_{CA-N-2}, $TS_{SUB-NO-2}$, and $TS_{SUB-N-2}$. Dashed lines indicate charge depletion ($\nabla^2\rho(\mathbf{r}) > 0$), solid lines indicate charge concentration ($\nabla^2\rho(\mathbf{r}) < 0$).
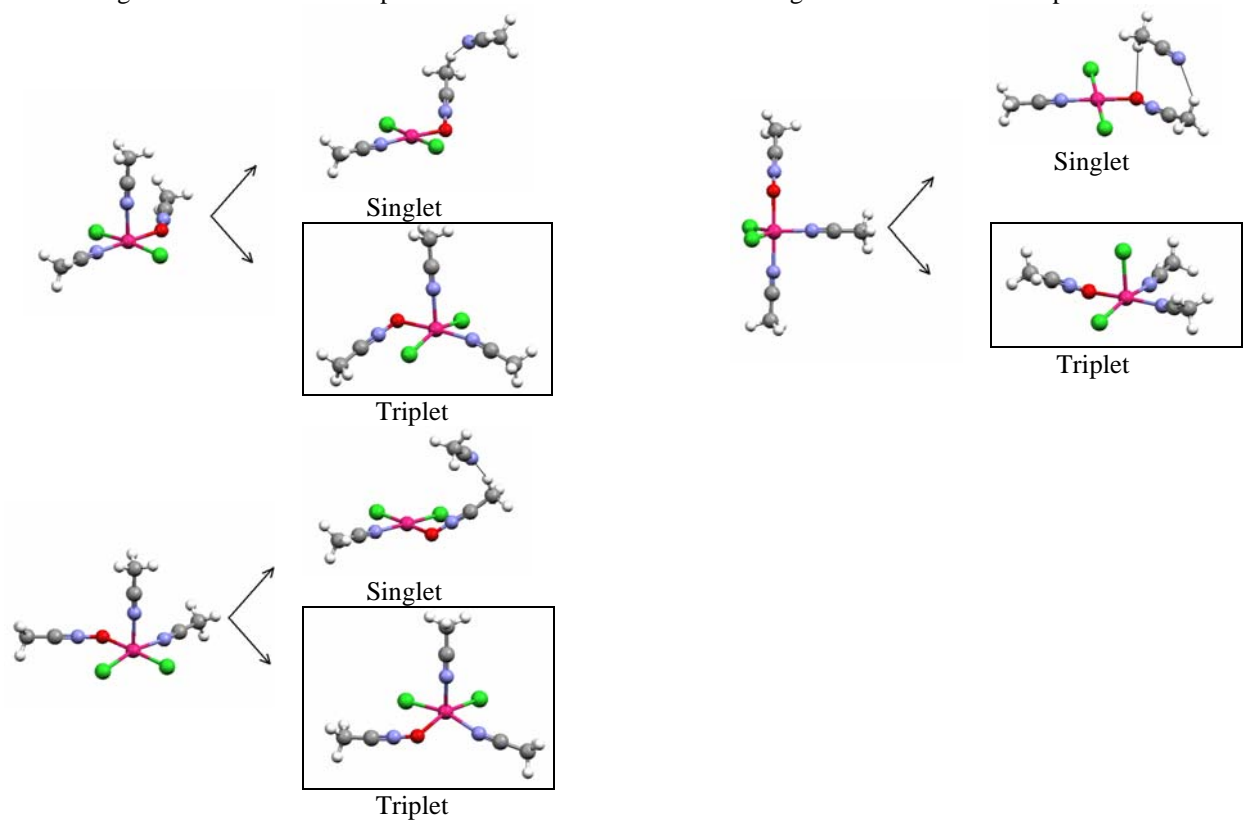
Starting structure   Optimized structure   Starting structure   Optimized structure

Singlet

Triplet

Singlet

Triplet

Singlet

Triplet

Singlet

Triplet

Singlet

Triplet

Singlet

Triplet

Singlet

Triplet

Singlet

Triplet

Starting structure   Optimized structure   Starting structure   Optimized structure

Singlet

Triplet

Singlet

Triplet

Singlet

Triplet
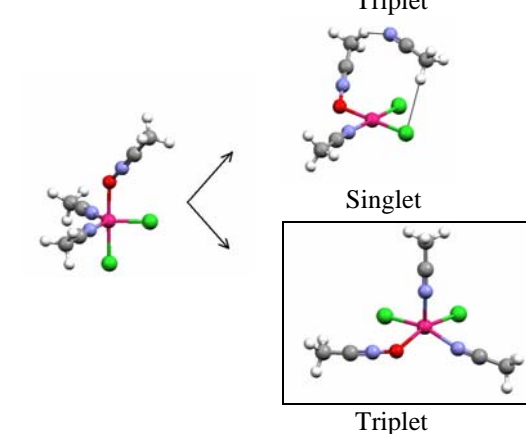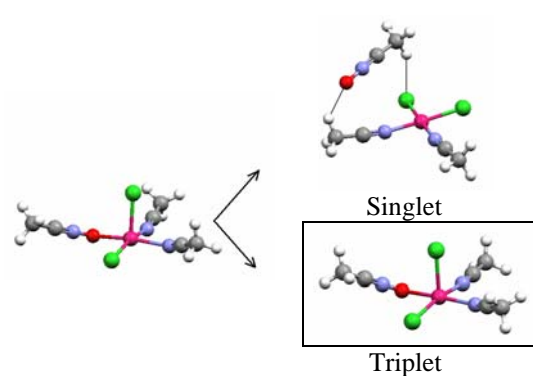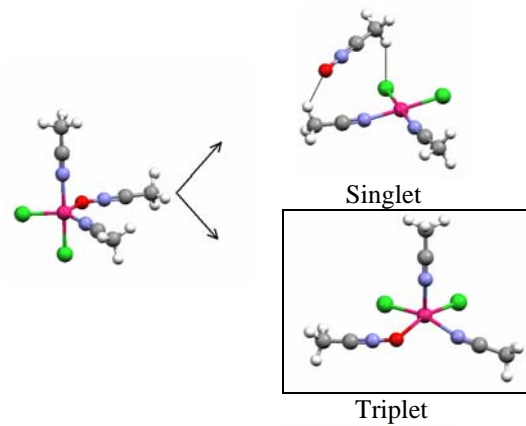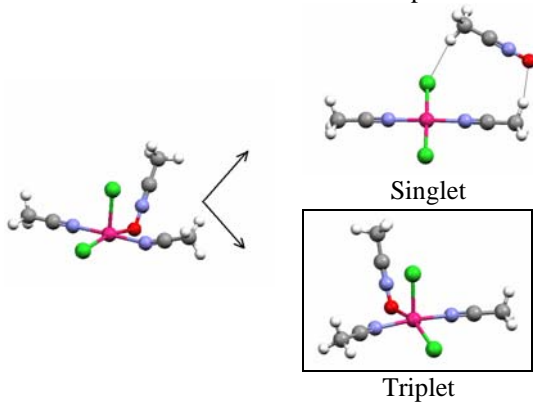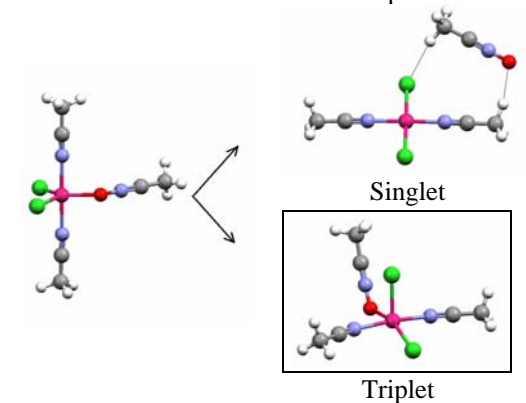
Figure 2S Starting structures used for the search of possible intermediates for the stepwise associative mechanism of the substitution reaction of **2** with CH$_3$C≡NO and corresponding optimized structures. Equilibrium structures of penta-coordinated intermediates are boxed.
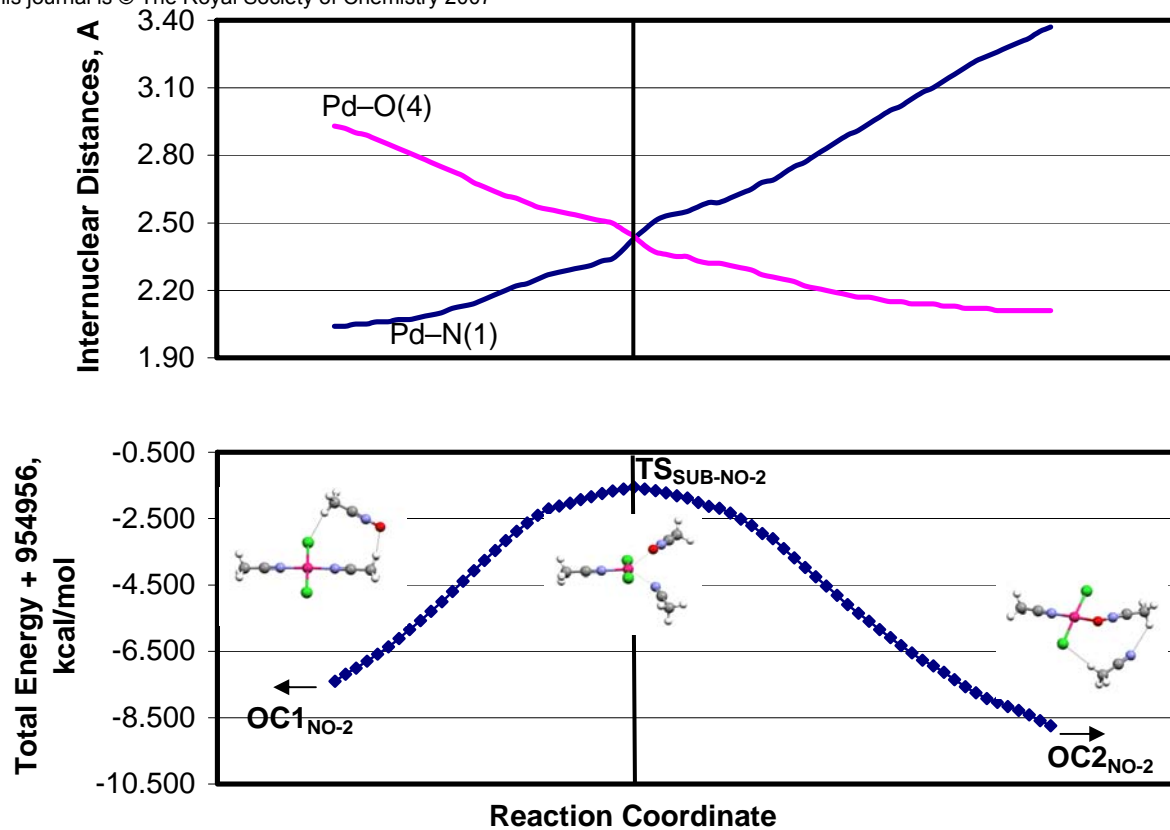
Figure 3S Calculated intrinsic reaction coordinate and change of Pd–O(4) and Pd–N(1) internuclear distances along the reaction path for the SUB reaction of **2** with $CH_3C{\equiv}NO$.